Static and dynamic behavior of PU foams with multilayer coatings

Available online at www.sciencedirect.com

ScienceDirect

Procedia Structural Integrity 19 (2019) 388–394

Structural Integrity Procedia

www.elsevier.com/locate/procedia

Fatigue Design 2019

# Static and dynamic behavior of PU foams with multilayer coatings

Francesca Curà[a], Raffaella Sesana[a]*, Fabrizio Scarpa[b], Xiao-Chong Zhang[b], Hua-Xin Peng[c]

[a]*DIMEAS, Politecnico di Torino, corso Duca degli Abruzzi 24, 10129 Torino, ITALY*
[b] *Bristol Composites Institute (ACCIS), University of Bristol, BS8 1TR Bristol, UK*
*c Institute for Composites Science Innovation (InCSI), School of Materials Science and Engineering, Zhejiang University, Hangzhou, 310027, PRC*

**Abstract**

An overview on static and dynamic behavior of functional polymeric foams is presented. In particular, a PU (Poly Urethane) open cells foam was manufactured to obtain specimens with different nanostructured coatings.
An experimental campaign was performed with 7 different kind of multilayer coatings.
Quasi-static compression preconditioning and compression fatigue cycles were applied and 5 parameters were measured during cycling: Hysteresis loop area, Dissipated energy per cycle, Stiffness degradation, Secant modulus, Loss factor values.
The results show the effect of the contribution of nanoink layers to the static and cyclic behavior of foams.


Peer-review under responsibility of the Fatigue Design 2019 Organizers.

*Keywords:* multilayer nanocomposites; nanoinks foams; mullin effect; hyperelasticity.

## 1. Introduction

Polymer nanocomposite foams combine the energy absorption and lightweight properties of foams, with the added multifunctionalities of nanomaterials dispersed within their structure, with enhanced strength (Dolomanova et al. (2011), Chen et al. (2014), Chen et al. (2011)) and dielectric properties (Chen et al. (2014), Athanasopoulos et al. (2012), Dai et al. (2012)), sound and vibration damping (Verdejo et al. 2009), Lee et al. (2012), Sung et al. (2007), Bandarian et al. (2011)), energy dissipation under compressive loading (Bezazi and Scarpa (2007)). This damping capacity is due to the energy dissipation mechanisms involved in the polymer/carbon nanotube (CNT) interface that is: nanotube/nanotube interfacial sliding and – in the case of multi-walled carbon nanotubes (MWCNTs) – the coaxial

2452-3216 
Peer-review under responsibility of the Fatigue Design 2019 Organizers.
10.1016/j.prostr.2019.12.042

sliding of the tube walls (Verdejo et al (2009), Zhang et al. (2014)); the formations of internal voids in the nanocomposite foam struts because of clustering and inhomogeneity (Bandarian et al. (2011)).

These examples refer to open cell foams made from the dispersion of nanoparticles within the chemical compounds used in the foaming process. In (Kang et al. (2007), Chen et al. (2015), Zhang et al (2016)) an alternative approach is proposed and described to produce these particular nanocomposite foams is by dip coating the porous materials in nanoinks. These procedures allow to obtain a multilayer structured composite foam with coating well adherent to the foam substrate. The microscopic investigation of damage phenomena related to cyclic loading of polymeric foams at the author's knowledge is poor. In Hu et al. (2018) an accurate microscopic analysis on the effect of cyclic compression on a metallic open cell foam with coating is applied to a metallic foam. The coating damage phenomena were described from a microscopic point of view in (Bandarian et al. (2011), Zhang et al. (2014), Zhang et al (2016)) where it was observed energy dissipation is related to nanotube-nanotube interfacial sliding of the tube walls within multiwall carbon nanotubes. However, to the author's knowledge, very few studies were performed on damage phenomena of multilayer composite nanocoated open cell polyurethane foams.

In the present paper an overview on static and dynamic behavior of functional polymeric foams is presented. In particular, A PU (Poly Urethane) open cells foam was cut to obtain specimens.

Different layers of coating were applied to the foam: two samples were coated with one layer (1PU) and 4 layers (4PU) of PUD (polyurethane dispersion) respectively, while 4 samples, after being coated with 1 layer PU, were coated with 1 layer (1MW), 2 layers (2MW), 3 layers (3MW) 4 layers (4MW) of CNT (carbon nanotube).

The tests aim at characterizing the materials behavior to calibrate the material constitutive models for future numerical simulations.

More in detail, experimental analysis entails at investigating the effect of foams coating on static and dynamic parameters when frequency and compression amplitude is varied from linear to non-linear elastic behavior.

Experimental procedures are defined according to International Standards. The following parameters were calculated by means of processing resulting data, for different number of cycles: the area of the hysteresis cycle, the dissipated energy per cycle, the secant modulus of the cycle, the stiffness degradation (rigidity loss) and the loss factor.

## 2. Materials and method

Seven different samples of materials were tested, one specimen per each material. A PU (Poly Urethane) open cells foam was cut to obtain specimens. Different layers of coating were applied to the foam: two samples were coated with one layer (1PU) and 4 layers (4PU) of PUD (polyurethane dispersion) respectively, while 4 samples, after being coated with 1 layer PU, were coated with 1 layer (1MW), 2 layers (2MW), 3 layers (3MW) 4 layers (4MW) of CNT (carbon nanotube). Each specimen was measured along the three main dimensions by means of a precision caliper. In Figure 1 the specimens are reported, in the same figure, the measurement directions are indicated.

Five specimens per material were used for quasi-static tests, one specimen per material was used for cyclic tests. Tests were run according to ASTM D4065. A preconditioning 5 cycle quasi-static loading was applied to 20% strain. Quasi-static preconditioning was run by means of a MTS QTest/10 testing machine, equipped with a 50 N load cell, in displacement control, with a 5 N preload and a maximum 20% strain. This value was selected to avoid the steep hardening phase in the stress-strain diagram. Then a sequence of 4 load blocks of 100000 cycles was applied to one specimen per sample: 0,5% strain and 1 Hz, 0,5% strain and 10 Hz, 1% strain and 1Hz and 1% strain and 10 Hz. These cycles were applied by means of a BOSE Electroforce 5500, load cell 200 N, in displacement control. Load [N] L and crosshead displacement [mm] $\Delta l$ were acquired during testing.

Nominal strain $\varepsilon$ was calculated as follows the ratio between crosshead displacement $\Delta l$ and specimen initial length $l_o$. Nominal stress $\sigma$ was calculated as the ratio between the load $L$ and the specimen initial cross section $A_0$.

Transversal deformation effects were neglected.

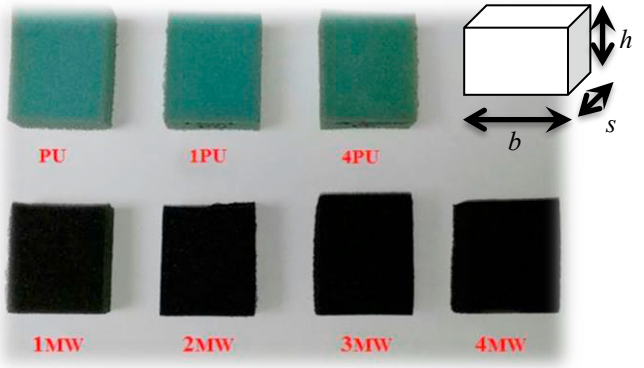


Fig. 1. specimen designation and main dimensions.

The following parameters were calculated by means of processing resulting data, for different number of cycles: the area of the hysteresis cycle, the dissipated energy per cycle, the secant modulus of the cycle, the stiffness degradation (rigidity loss) and the loss factor.

The hysteresis cycle area was calculated by means of numerical integration by means of the trapezium rule (Davis and Rabinowitz (2007)) on the stress-strain diagram as already done in Curà and Sesana (2014).

The dissipated energy is assumed to be related to the hysteresis cycle area (Lazan (1968)) for elastic materials; then it was obtained as the area of the hysteresis cycles times the specimen volume.

The secant modulus was calculated as the ratio between the difference of maximum and minimum stress and the difference between the corresponding maximum and minimum strain of the cycle for hysteresis cycles with elliptical shape.

The stiffness degradation *SD* was calculated as the ratio between the maximum stress in a cycle and the maximum stress that of the first cycle.

The loss factor $\eta$ was calculated as the ratio between *D*, the energy dissipated per cycle (or the energy that must be supplied to the system to maintain steady state conditions) and *W*, the total (kinetic plus potential) energy associated with the vibration time $2\pi$ (Ungar and Kerwin (1962)):

$$\eta = \frac{D}{2\pi W}$$

## 3. Results and discussion

The results of quasi-static cyclic preconditioning of specimens are reported in Figure 2 and 3. In Figure 2 the 5 preconditioning cycles are reported for pure material PU, for 4PU and 4MW specimens as an example. The change in slope between the two linear trends occurs for strain values about 5%. Increasing the number of coating layers increases the maximum stress and the area of the hysteresis cycle.

Figure 3 shows the average decrement $\Delta\sigma_{max}$ of the maximum stress $\sigma_{max}$ on five specimens per material from the first to the fifth cycle in quasi-static cycling (Figure 3*a*). The same value, normalized with respect to the maximum stress in the first cycle and in % value, $\%\Delta\sigma_{norm}$, is also reported (Figure 3*b*). It can be observed that this decrement of maximum stress (stress softening) corresponds to the hyperelastic behavior described by Mullin effect (Govindjee and Simo (1991), Ogden and Roxburg (1999)).

This means that damage phenomena are taking place during uniaxial static compression. The contribution to damage may be split in two parts, the first part can be accounted to pure foam (PU) and it is constant for all specimens; the second one can be attributed to coating layers damage (Bandarian et al (2011), Zhang et al (2016), Zhang et al (2016)).

This second contribution is quantitatively different for different specimens as demonstrated from the analysis of Figure 3. Similar results can be found in cyclic experiments.

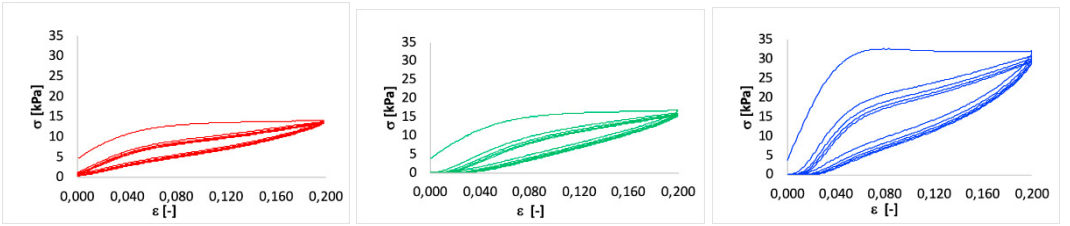


Figure 2: average hysteresis cycles for PU (a) specimen, 4PU (b) and 4MW (c) specimens in quasi-static cycling

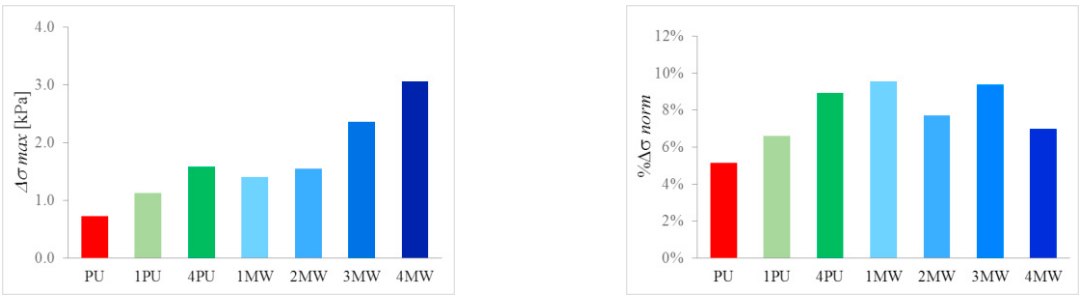


Figure 3: average decrement in maximum stress in absolute value *(a)* and % normalized (b) in quasi-static cycling

From the analysis of Figure 3 it can be observed that the presence of different coating layers strongly influences the foams behavior, providing in all cases a stiffening effect. This behavior changes substantially during the quasi-static cyclic preconditioning; in particular, PU layers show a linear decrement in maximum stress by increasing the number of layers, while MW layers show a higher degradation that appears to not be influenced by the layers number increasing.

In the following Tables 1-3 the results of the experimental cyclic tests are reported. In particular in Table 1 the stiffness degradation, in Table 2 the secant modulus, in Table 3 the loss factor. The area of the hysteresis cycle and the dissipated energy per cycle were used to calculate the loss factor values.

Table 1. Stiffness degradation [-].

| | PU | 1PU | 4PU | 1MW | 2MW | 3MW | 4MW |
|---|---|---|---|---|---|---|---|
| 1% 1 Hz | 0,078 | 0,116 | 0,322 | 0,256 | 0,237 | 0,228 | 0,101 |
| 1% 10 Hz | 0,196 | 0,225 | 0,252 | 0,207 | 0,207 | 0,232 | 0,212 |
| 0,5% 1 Hz | 0,237 | 0,349 | 0,328 | 0,323 | 0,374 | 0,075 | 0,119 |
| 0,5 % 10 Hz | 0,169 | 0,268 | 0,288 | 0,230 | 0,264 | 0,293 | 0,194 |

Table 2. Secant modulus [kPa].

| | PU | 1PU | 4PU | 1MW | 2MW | 3MW | 4MW |
|---|---|---|---|---|---|---|---|
| 1% 1 Hz | 15034,3 | 30483,3 | 12614,9 | 3661,7 | 3537,0 | 3466,2 | 19492,0 |
| 1% 10 Hz | 10155,9 | 4554,2 | 15507,4 | 40279,0 | 2431,9 | 15695,7 | 98802,5 |
| 0,5% 1 Hz | 18653,7 | 22124,5 | 53449,1 | 27728,4 | 18286,3 | 47237,8 | 13994,6 |
| 0,5 % 10 Hz | 5626,6 | 3885,9 | 4329,0 | 13818,7 | 15626,1 | 24211,9 | 1842,3 |

Table 3. Loss factor [-].

| | PU | 1PU | 4PU | 1MW | 2MW | 3MW | 4MW |
|---|---|---|---|---|---|---|---|
| 1% 1 Hz | 0,257 | 0,078 | 0,058 | 0,247 | 0,187 | 0,183 | 0,271 |
| 1% 10 Hz | 0,011 | 0,023 | 0,012 | 0,167 | 0,085 | 0,086 | 0,355 |
| 0,5% 1 Hz | 0,017 | 0,009 | 0,001 | 0,007 | 0,004 | 0,036 | 0,103 |
| 0,5 % 10 Hz | 0,015 | 0,003 | 0,010 | 0,004 | 0,003 | 0,006 | 0,002 |

In Figure 4 and 5, as an example, the values of stiffness degradation to evaluate the effect of the PU and CNT coatings in different strain and frequency conditions are reported. In Figure 6 and 7 analogous results are shown for Loss factor.

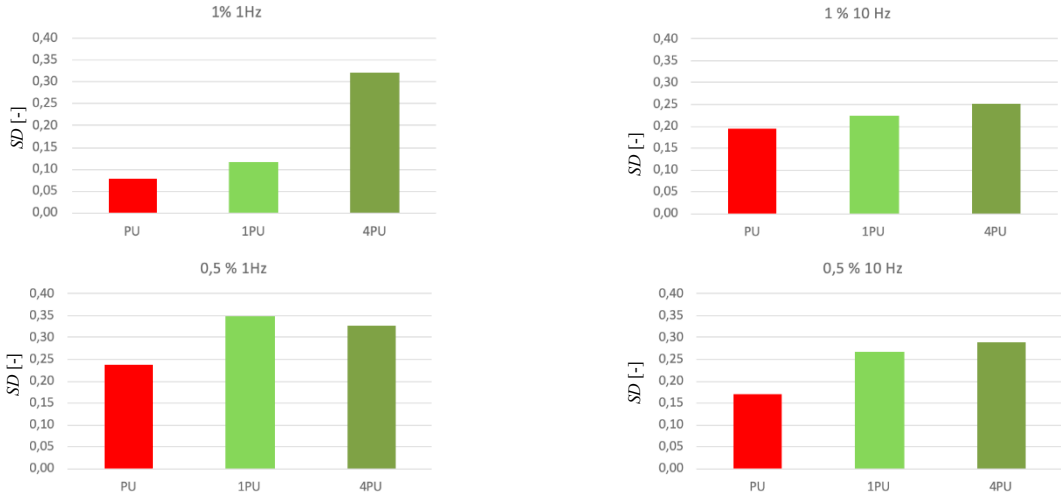


Fig. 4. Stiffness degradation in different strain and frequency conditions for different number of PU coating layers.

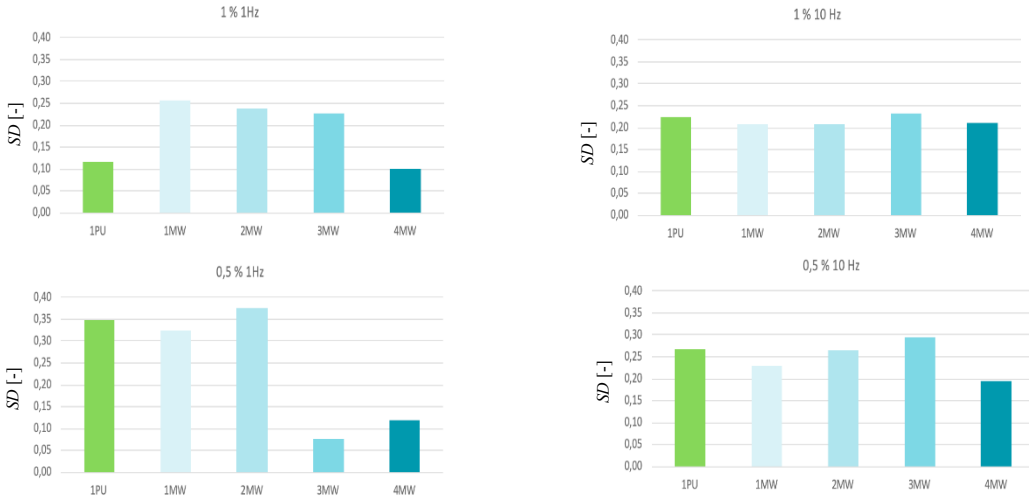


Fig. 5. Stiffness degradation in different strain and frequency conditions for different number of CNT coating layers.


Fig. 6. Loss factor in different strain and frequency conditions for different number of PU coating layers.

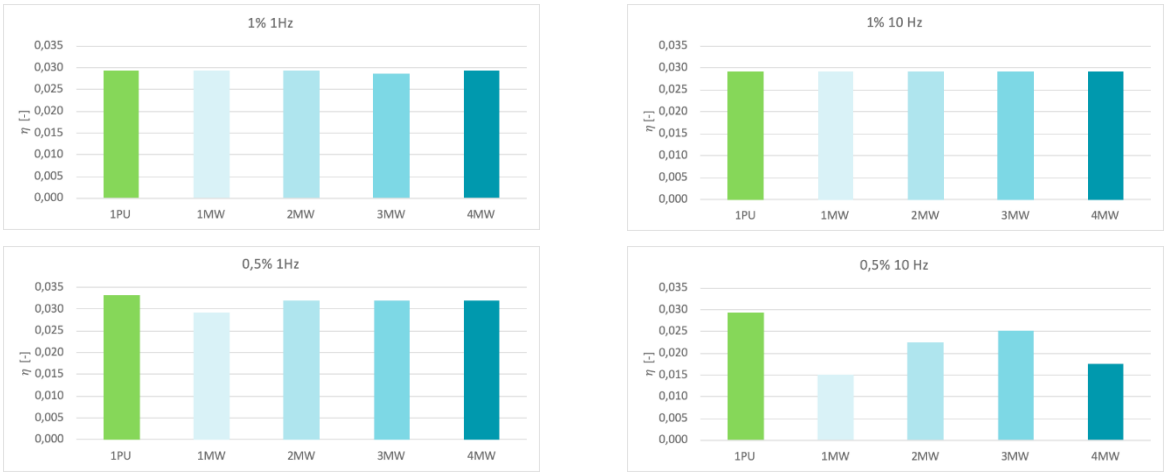


Fig. 7. Loss factor in different strain and frequency conditions for different number of CNT coating layers.

From the analysis of Figures 4-7 it can be observed that the test frequency influences the foams characteristics.

For 10 Hz and higher strain, differences in stiffness degradation (see Figures 4 and 5) between coated and uncoated specimens become lower, regardless the kind of coating, PU or CNT.

In Figures 6 and 7 higher loss factor values can be observed for higher strains. The influence of the test frequency doesn't appear in these first results.

For this kind of foams, a plateau is usually reached for 5% strain and then the loss factor tends to decrement for high strains. In this case of lower % values of strain, probably other effects are presents in the case of coated foams, to affect the behavior of loss factor.

## 4. Conclusions

In the present paper the results of an experimental activity on multilayer nanocoated PU open cell foams are presented. Quasi-static and cyclic compression tests were performed. The particular aim was to characterize the effect of different number and kind of layers: PU and CNT nanoinks.

The results of quasi-static cyclic preconditioning of specimens show that an increasing number of coating layers increases the maximum stress and the area of the hysteresis cycle.

It can also be observed for all specimens a decrement in the maximum stress with cycles (stress softening) and this phenomenon is more evident increasing the number of layers. This difference in damaging behavior can be attributed to the coating layer contribution. This trend is linear for PU layers and non-linear for MW layers.

For cyclic characterization the following parameters, obtained from the hysteresis loops, were chosen: Stiffness degradation, Secant modulus and Loss factor.

From this first analysis, it appears that both strain amplitude and test frequency influence the foams characteristics.

Further tests will validate from a quantitative point of view these evidences.

## References

Athanasopoulos, N., A. Baltopoulos, A., M. Matzakou, M., Vavouliotis, A., Kostopoulos, V., 2012. Electrical conductivity of polyurethane/MWCNT nanocomposite foams. Polym Composite 33(8), 1302-1312.

Bandarian, M., Shojaei, A., Rashidi, A.M., 2011. Thermal, mechanical and acoustic damping properties of flexible open-cell polyurethane/multi-walled carbon nanotube foams: effect of surface functionality of nanotubes. Polym Int, 60(3), 475-482.

Bezazi, A., Scarpa, F., 2007. Mechanical behaviour of conventional and negative Poisson's ratio thermoplastic polyurethane foams under compressive cyclic loading. International Journal of fatigue 29, 922-930.

Chen, L.M., Schadler, L.S., Ozisik, R., 2011. An experimental and theoretical investigation of the compressive properties of multi-walled carbon nanotube/poly(methyl methacrylate) nanocomposite foams. Polymer, 52(13), 2899-2909.

Chen, M.T., Zhang, L., Duan, S.S., Jing, S.L., Jiang, H., Luo, M.F., Li, C.Z.2014. Highly conductive and flexible polymer composites with improved mechanical and electromagnetic interference shielding performances. Nanoscale 6(7), 3796-3803.

Chen, Y.J., Li, Y., Chu, B.T.T., Kuo, I.T., Yip, M., Tai, N., 2015. Porous composites coated with hybrid nano carbon materials perform excellent electromagnetic interference shielding. Composites: Part B , 70, 231-237.

Curà, F., Sesana, R., 2014. Mechanical and thermal parameters for high-cycle fatigue characterization in commercial steels. Fatigue Fract Engng Mater Struct 37, 883–896.

Dai, K., Ji, X., Xiang, Z.D., Zhang, W.Q., Tang, J.H., Li, Z.M., 2012. Electrical Properties of an Ultralight Conductive Carbon Nanotube/Polymer Composite Foam Upon Compression. Polym-Plast Technol, 51(3), 304-306.

Davis, P. J., Rabinowitz, P., 2007. Methods of Numerical Integration Dover Books on Mathematics Series. Dover Publications, Inc, Mineola, N.Y.

Dolomanova, V., Rauhe, J.C.M., Jensen, L.R., Pyrz, R., Timmons, A.B. 2011. Mechanical properties and morphology of nano-reinforced rigid PU foam. Journal of Cellular Plastics. J Cell Plast 47(1), 81-93.

Govindjee, S., Simo, S., 1991. A micro-mechanically based continuum damage model for carbon black-filled rubbers incorporating Mullins' effect, J. Mech. Phys. Solids 39(I), 87-112.

Hu, Z.L., Pang, Q., Ji, G.Q., Wu, G.H., 2018. Mechanical behaviors and energy absorption properties of Y/Cr and Ce/Cr coated open-cell nickel-based alloy foams. Rare Met. 37(8), 650-661.

Kang, T., Yoon, J., Kim, D., Kum, S., Huh, Y., Hahn, J., Moon, S., Lee, H., Kim, Y., 2007. Sandwich-Type Laminated Nanocomposites Developedby Selective Dip-Coating of Carbon Nanotubes. Adv. Mater 19, 427-432.

Lazan, B. J., 1968. Damping of materials and members in structural mechanics (Oxford Pergamon Press Oxford).

Lee, J., Kim, G.H., Ha, C.S., 2012. Sound Absorption Properties of Polyurethane/Nano-Silica Nanocomposite Foams. J Appl Polym Sci, 123(4), 2384-2390.

Ogden, R.W., Roxburgh, D.G. 1999. A pseudo–elastic model for the Mullins effect in filled rubberProceedings of the Royal Society of London. 455, 2861–2877.

Sung, C.H., Lee, K.S., Lee, K.S., Oh, S.M., Kim, J.H., Kim, M.S., Jeong, R.M., 2007. Sound damping of a polyurethane foam nanocomposite. Macromol Res, 15(5), 443-448.

Verdejo, R., Stämpfli, R., Alvarez-Lainez, M., Mourad, S., Rodriguez-Perez, M.A., Brühwiler, P.A., Shaffer, M., 2009. Enhanced acoustic damping in flexible polyurethane foams filled with carbon nanotubes. Compos Sci Technol, 69(10), 1564-1569.

Ungar, E.E., Kerwin, E.M. 1962. Loss factors of viscoelastic systems in terms of energy concepts. The Journal of the Acoustical Society of America, 34(7), 954-957.

Zhang, X.C., Peng, H.X., Limmack, A.P., Scarpa, F., 2014. Viscoelastic damping behaviour of cup stacked carbon nanotube modified epoxy nanocomposites with tailored interfacial condition and re-agglomeration. Compos Sci Technol, 105, 66-72.

Zhang, X.C., Scarpa, F., McHale, R., Limmack, A.P., Peng, H.X., 2016. Carbon nano-ink coated open cell polyurethane foam with micro-architectured multilayer skeleton for damping applications. RSC Advances, 6(83), 80334-80341.